Scientific Research Publishing

Journal of Applied Mathematics and Physics, 2022, 10, 3920-3936
https://www.scirp.org/journal/jamp
ISSN Online: 2327-4379
ISSN Print: 2327-4352

Quintic B-Spline Method for Solving Sharma Tasso Oliver Equation

Talaat S. Eldanaf[1], Mohamed Elsayed[2], Mahmoud A. Eissa[1], Faisal Ezz-Eldeen Abd Alaal[3]

[1]Department of Mathematics and Computer Science, Faculty of Science, Menoufia University, Shebin El-Kom, Egypt
[2]Basic Science Department, School of Engineering, Canadian International College "CIC", Giza, Egypt
[3]Department of Mathematics, Faculty of Science, Damanhour University, Damanhour, Egypt
Email: tdanaf@taibahu.edu.sa, mzaki.math@yahoo.com, mahmoud.eisa@science.menofia.edu.eg, m.eissa@hit.edu.cn, faisalezz@sci.dmu.edu.eg

How to cite this paper: Eldanaf, T.S., Elsayed, M., Eissa, M.A. and Alaal, F.E.-E.A. (2022) Quintic B-Spline Method for Solving Sharma Tasso Oliver Equation. *Journal of Applied Mathematics and Physics*, **10**, 3920-3936.
https://doi.org/10.4236/jamp.2022.1012258

Received: October 29, 2022
Accepted: December 27, 2022
Published: December 30, 2022

Abstract

When analysing the thermal conductivity of magnetic fluids, the traditional Sharma-Tasso-Olver (STO) equation is crucial. The Sharma-Tasso-Olive equation's approximate solution is the primary goal of this work. The quintic B-spline collocation method is used for solving such nonlinear partial differential equations. The developed plan uses the collocation approach and finite difference method to solve the problem under consideration. The given problem is discretized in both time and space directions. Forward difference formula is used for temporal discretization. Collocation method is used for spatial discretization. Additionally, by using Von Neumann stability analysis, it is demonstrated that the devised scheme is stable and convergent with regard to time. Examining two analytical approaches to show the effectiveness and performance of our approximate solution.

Keywords

Nonlinear Partial Differential Equations, Sharma-Tasso-Olver (STO) Equation, Quintic B-Spline Collocation Method, Von Neumann Stability Analysis

1. Introduction

Numerical Analysis is considered an important branch in mathematics which plays an important solution in finding an approximate solution for feature nonlinear PDEs which has no exact solution. Most numerical solution depends on interpolation and spline interpolation plays an important base in polynomial interpolation in most mathematical branches such as numerical analysis, computation, integration, differentiation, etc. Many physicists and mathematicians have paid their attentions to the Sharma-Tasso-Olver (STO) equation in recent years due to its appearance in scientific applications. The researchers who solved the Sharma-Tasso-Olver (STO) equation include Wazwaz (2007) who used the tanh method, the extended tanh method, and other ansatz involving hyperbolic and exponential functions efficiently used for the analytic study of this equation [1]. In [2], Yan investigated the Sharma-Tasso-Olver Equation (1) by using the Cole-Hopf transformation method. The simple symmetry reduction procedure is used in [3] to obtain exact solutions where soliton fission and fusion have been examined. Wang *et al.* examined the soliton fission and fusion thoroughly by means of the Hirotas bilinear method and the Bäcklund transformation method in [4]. The generalized Kaup-Newell-type hierarchy of nonlinear evolution equations is explicitly related to Sharma-Tasso-Olver equation from [5]. Chao Yue in [6] provided theta function representation of algebro-geometric solutions and related crucial quantities for the complex Sharma-Tasso-Olver (CSTO) hierarchy. In [7] the simple symmetry reduction procedure is repeated by examining soliton fission and fusion to obtain the exact solutions for STO. Using the improved tanh function method in [8], the Sharma-Tasso-Olver equation with its fission and fusion has some exact solutions. In 2006 Klaus *et al.* developed the instability of algebraic solitons for integrable nonlinear equations in one spatial dimension that include modified KdV, focusing NLS, derivative NLS, and massive Thirring equations [8] [9]. In [9], the Korteweg-de Vries-Burgers' (KdVB) equation is solved numerically by a new differential quadrature method based on quintic B-spline functions. In [10] S. I. Zaki introduced the quintic B-spline finite elements scheme for the KdVB equation. R.C. Mittal and R.K. Jain discussed a collocation method for solving some Rosenau type non-linear higher in [11]. In [12] H. Tariq and G. Akram solved the fourth-order partial differential equations with Caputo time fractional derivative on a finite domain with quintic polynomial spline technique. Krwan Jwame and Najim Abdullah developed the B-spline method for solving higher order differential equations in [13]. In [14], K. R Raslan *et al.* proposed the numerical solution of a coupled system of Burgers' equation by using the quintic B-spline collocation scheme on the uniform mesh points. Ding and Wong solved a time-fractional nonlinear Schrödinger equation by using the quintic non-polynomial spline in [15]. In 1946, J. H. Ahlberg [16] introduced spline functions. Mathematically, a spline function consists of polynomial pieces on sub intervals joined together with certain continuity conditions. Second order linear two-point boundary value problems were solved using extended cubic B-spline interpolation method by Hamid *et al.* in 2011 [17]. In the same year, Eisa *et al.* used uniform quartic spline polynomial functions to develop some consistency relations, which are then used to derive a numerical method for approximating the solution [18]. In 2006, Caglar *et al.* considered the B-spline interpolation and compares this method with finite difference, finite element and finite volume methods which applied to the two-point boundary value problem [19]. Fauzi and Sulaiman, discussed the application of

Half-Sweep Modified Successive Over Relaxation (HSMSOR) iterative method for solving second order two-point boundary value problems [20]. Recently, in 2021 Hadhoude *et al.* showed how to approximate the solution to the generalized time-fractional Huxley Burgers' equation by a numerical method based on the cubic B-spline collocation method and the mean value theorem for integrals [21]. Next year, Hadhoude *et al.* introduced the cubic non-polynomial spline functions to develop a computational method for solving the fractional modified Burgers' equation [22], Mustafa Inc and, Zeliha S Korpinar, Maysaa, Mohamed Al Qurashi and Dumitru Baleanu, introduced numerical solutions by Residual power series method of the sharma Tasso Oliver equation [23]. Doğan Kaya *et al.* compared exact and numerical Solutions for the Sharma-Tasso-Olver Equation [24]. Alzaid, N. and Alrayiqi, B. introduced Adomian decomposition method (ADM) implemented to approximate the solution of the KdV equations of the seventh order, which are Kaup-Kuperschmidt equation and seventh order Kawahara equation, the ADM is very efficient [25]. An, J. and Guo, X. discussed the numerical solution of the boundary value problem that is two-order fuzzy linear differential equations [26].

This paper is designed to determine the approximate solution of Sharma-Tasso-Olive (STO) equation. The approximate solution is based on forward difference formula and B-spline collocation method. The paper is divided into four sections. The quintic B-spline basis function was given in Section 2. The stability and convergence analysis using the Von-Neumann method is discussed in Section 3. In Section 4 we apply an illustration example to discuss the applicability of our designed method.

The generalized STO equation [1] [2] [3] is defined as:

$$\frac{\partial U}{\partial t}+3\alpha U_x^2+3\alpha U^2U_x+3\alpha UU_{xx}+\alpha U_{xxx}=0 \tag{1.1}$$

where, α is a parameter that $\alpha>0$.

2. Description of Method

In quintic B-splines collocation method the approximate solution which is obtained as a linear combination of quintic B-spline basis functions $\phi_i(x)$ approximation space under consideration and undetermined coefficients $w_i(t)$, From the above basis, the approximation solution $U_n(x,t)$ can be written in terms of linear combination of quentic B-Spline base function as follows:

$$U_n(x,t)=\sum\nolimits_{i=-2}^{n+2}\phi_i(x)w_i(t) \tag{2.1}$$

And its derivatives be in the form:

$$U_t=\sum\nolimits_{i=-2}^{n+2}\phi_i(x)w_i'(t),\quad U_x=\sum\nolimits_{i=-2}^{n+2}\phi_i'(x)w_i(t) \tag{2.2}$$

$$U_{xx}=\sum\nolimits_{i=-2}^{n+2}\phi_i''(x)w_i(t),\quad U_{xxx}=\sum\nolimits_{i=-2}^{n+2}\phi_i'''(x)w_i(t) \tag{2.3}$$

In our work, we will use the quintic B-spline polynomial as a base function to construct the approximate solution. quintic splines defined as follow:

$$\phi_i(x)=\frac{1}{h^5}\begin{cases}(x-x_{i-3})^5 & x\in[x_{i-3},x_{i-2}]\\ (x-x_{i-3})^5-6(x-x_{i-2})^5 & x\in[x_{i-2},x_{i-1}]\\ (x-x_{i-3})^5-6(x-x_{i-2})^5+15(x-x_{i-1})^5 & x\in[x_{i-1},x_i]\\ (x-x_{i-3})^5-6(x-x_{i-2})^5+15(x-x_{i-1})^5-20(x-x_i)^5 & x\in[x_i,x_{i+1}]\\ (x-x_{i-3})^5-6(x-x_{i-2})^5+15(x-x_{i-1})^5-20(x-x_{i+1})^5 & x\in[x_{i+1},x_{i+2}]\\ (x-x_{i-3})^5-6(x-x_{i-2})^5+15(x-x_{i-1})^5-20(x-x_{i+1})^5-6(x-x_{i+2})^5 & x\in[x_{i+2},x_{i+3}]\\ 0 & \text{otherwise.}\end{cases}$$

where $h=x_i-x_{i-1}$, then the quintic spline function and its derivatives at nodes x_i defined as in Table 1 as follows:

By substitution in Equations (2.1) and (2.2), with the values of the U,U',U'',U''' at nodel points determined in terms of w_i can be written by:

$$\begin{aligned}U(x_i)&=w_{i-2}^n+26w_{i-1}^n+66w_i^n+26w_{i+1}^n+w_{i+2}^n\\ U_x(x_i)&=\frac{5}{h}\{-w_{i-2}-10w_{i-1}+10w_{i+1}+w_{i+2}\}\\ U_{xx}(x_i)&=\frac{20}{h^2}\{w_{i-2}+2w_{i-1}-6w_i+2w_{i+1}+w_{i+2}\}\\ U_{xxx}(x_i)&=\frac{60}{h^3}\{w_{i-2}-2w_{i-1}+2w_{i+1}-w_{i+2}\}\end{aligned}\tag{2.4}$$

Also we can define:

$$w_i^n=\frac{w_i^{n+1}+w_i^n}{2},\quad \left(w_i^n(t)\right)'=\frac{w_i^{n+1}-w_i^n}{k}$$

$$U_x^2=U_xU_x\tag{2.5}$$

On substituting global approximation (2.1) and its necessary derivatives (2.2) in (1.1), following set of the first order ordinary differential equations is obtained as,

$$\begin{aligned}&\sum_{i=-2}^{n+2}\phi_i(x)w_i'(t)+3\alpha\left(\sum_{i=-2}^{n+2}\phi_i'(x)w_i(t)\right)^2+3\alpha\sum_{i=-2}^{n+2}\phi_i'(x)w_i(t)*\left(\sum_{i=-2}^{n+2}\phi_i(x)w_i(t)\right)^2\\ &+3\alpha\left(\sum_{i=-2}^{n+2}\phi_i(x)w_i(t)\right)\left(\sum_{i=-2}^{n+2}\phi_i''(x)w_i(t)\right)+\alpha\sum_{i=-2}^{n+2}\phi_i'''(x)w_i(t)=0\end{aligned}$$

Then the equation takes the form:

Table 1. The values of ϕ_i and its derivatives at the knots.

	x_{i-2}	x_{i-1}	x_i	x_{i+1}	x_{i+2}
$\phi_i(x)$	1	26	66	26	1
$\phi_i'(x)$	$5/h$	$50/h$	0	$-50/h$	$-5/h$
$\phi_i''(x)$	$20/h^2$	$40/h^2$	$-120/h^2$	$40/h^2$	$20/h^2$
$\phi_i'''(x)$	$-60/h^3$	$120/h^3$	0	$120/h^3$	$60/h^3$

$$\frac{1}{k}\sum_{i=-2}^{n+2}\phi_i(x)\left(w_i^{n+1}-w_i^n\right)+3\alpha\sum_{i=-2}^{n+2}\phi_i'(x)\left(\frac{w_i^{n+1}+w_i^n}{2}\right)\left(\sum_{k=-2}^{n+2}\phi_k'(x)w_k\right)$$
$$+3\alpha\sum_{i=-2}^{n+2}\phi_i'(x)\left(\frac{w_i^{n+1}+w_i^n}{2}\right)\left(\sum_{k=-2}^{n+2}\phi_k(x)w_k\right)^2$$
$$+3\alpha\sum_{i=-2}^{n+2}\phi_i''(x)\left(\frac{w_i^{n+1}+w_i^n}{2}\right)\left(\sum_{k=-2}^{n+2}\phi_k(x)w_k\right)$$
$$+\alpha\sum_{i=-2}^{n+2}\phi_i'''(x)\left(\frac{w_i^{n+1}+w_i^n}{2}\right)=0$$

Let we define:

$$Z_k=\sum_{k=-2}^{n+2}\phi_k(x)w_k=w_{i-2}^n+26w_{i-1}^n+66w_i^n+26w_{i+1}^n+w_{i+2}^n$$
$$\gamma_k=\sum_{k=-2}^{n+2}\phi_k'(x)w_k=-\frac{5}{h}\left(w_{i-2}^n+10w_{i-1}^n-10w_{i+1}^n-w_{i+2}^n\right) \tag{2.6}$$

So the D.E be:

$$\frac{1}{k}\sum_{i=-2}^{n+2}\phi_i(x)\left(w_i^{n+1}\right)+\frac{3\alpha}{2}\sum_{i=-2}^{n+2}\phi_i'(x)\gamma_k w_i^{n+1}+\frac{3\alpha}{2}\sum_{i=-2}^{n+2}\phi_i'(x)\left(Z_k^2\right)w_i^{n+1}$$
$$+\frac{3\alpha}{2}\sum_{i=-2}^{n+2}\phi_i''(x)Z_k w_i^{n+1}+\frac{\alpha}{2}\sum_{i=-2}^{n+2}\phi_i'''(x)w_i^{n+1}$$
$$=\frac{1}{k}\sum_{i=-2}^{n+2}\phi_i(x)\left(w_i^n\right)-\frac{3\alpha}{2}\sum_{i=-2}^{n+2}\phi_i'(x)\gamma_k w_i^n-\frac{3\alpha}{2}\sum_{i=-2}^{n+2}\phi_i'(x)\left(Z_k^2\right)w_i^n$$
$$-\frac{3\alpha}{2}\sum_{i=-2}^{n+2}\phi_i''(x)Z_k w_i^n-\frac{\alpha}{2}\sum_{i=-2}^{n+2}\phi_i'''(x)w_i^n \tag{2.7}$$

So we can represent the components of the general solution $U(x,t)$ and its derivatives by using Table 1 for the coefficients for $\phi_i',\phi_i'',\phi_i'''$:

$$\left(w_{i-2}^{n+1}+26w_{i-1}^{n+1}+66w_i^{n+1}+26w_{i+1}^{n+1}+w_{i+2}^{n+1}\right)$$
$$+\left(\frac{3\alpha k}{2}*-\frac{5}{h}\right)\left(Z_k^2+\gamma_k\right)\left(w_{i-2}^{n+1}+w_{i-1}^{n+1}+w_{i+1}^{n+1}+w_{i+2}^{n+1}\right)$$
$$+\left(\frac{3\alpha k}{2}*\frac{20}{h^2}\right)\left(Z_k\right)\left(w_{i-2}^{n+1}+2w_{i-1}^{n+1}-6w_i^{n+1}+2w_{i+1}^{n+1}+w_{i+2}^{n+1}\right)$$
$$+\left(\frac{\alpha k}{2}*\frac{-60}{h^3}\right)\left(-w_{i-2}^{n+1}+2w_{i-1}^{n+1}-2w_{i+1}^{n+1}+w_{i+2}^{n+1}\right)$$
$$=w_{i-2}^n+26w_{i-1}^n+66w_i^n+26w_{i+1}^n+w_{i+2}^n$$
$$-\left(\frac{3\alpha k}{2}*-\frac{5}{h}\right)\left(Z_k^2+\gamma_k\right)\left(w_{i-2}^n+w_{i-1}^n+w_{i+1}^n+w_{i+2}^n\right)$$
$$-\left(\frac{3\alpha k}{2}*\frac{20}{h^2}\right)\left(Z_k\right)\left(w_{i-2}^n+2w_{i-1}^n-6w_i^n+2w_{i+1}^n+w_{i+2}^n\right)$$
$$-\left(\frac{\alpha k}{2}*\frac{-60}{h^3}\right)\left(-w_{i-2}^n+2w_{i-1}^n-2w_{i+1}^n+w_{i+2}^n\right)$$

After simplifying the previous equation we will get the following system of equations:

$$a_i w_{i-2}^{n+1}+b_i w_{i-1}^{n+1}+c_i w_i^{n+1}+d_i w_{i+1}^{n+1}+e_i w_{i+2}^{n+1}$$
$$=A_i w_{i-2}^n+B_i w_{i-1}^n+C_i w_i^n+D_i w_{i+1}^n+E_i w_{i+2}^n \tag{2.8}$$

where $a_i, b_i, c_i, d_i, e_i, A_i, B_i, C_i, D_i$ and E_i given as follows:

$$\begin{aligned}
&a_i = \left(1 - r_1\left(\gamma_k + Z_k^2\right) + r_2 Z_k + r_3\right),\ A_i = \left(1 + r_1\left(\gamma_k + Z_k^2\right) - r_2 Z_k - r_3\right) \\
&b_i = \left(26 - 2r_1\left(\gamma_k + Z_k^2\right) + 2r_2 Z_k - 2r_3\right),\ B_i = \left(26 + 2r_1\left(\gamma_k + Z_k^2\right) - 2r_2 Z_k + 2r_3\right) \\
&c_i = \left(66 - 6r_2 Z_k\right),\ C_i = \left(66 + 6r_2 Z_k\right) \\
&d_i = \left(26 + 2r_1\left(\gamma_k + Z_k^2\right) + 2r_2 Z_k + 2r_3\right),\ D_i = \left(26 - 2r_1\left(\gamma_k + Z_k^2\right) - 2r_2 Z_k - 2r_3\right) \\
&e_i = \left(1 + r_1\left(\gamma_k + Z_k^2\right) + r_2 Z_k - r_3\right),\ E_i = \left(1 - r_1\left(\gamma_k + Z_k^2\right) - r_2 Z_k + r_3\right) \\
&\text{and } r_1 = \frac{15\alpha k}{2h},\ r_2 = \frac{30\alpha k}{h^2},\ r_3 = \frac{30\alpha k}{h^3}
\end{aligned} \tag{2.9}$$

For this purpose, we will use initial and boundary conditions. Then the system of linear equation with $N + 3$ unknown for expression (2.4) becomes:

$$PY^{n+1} = QY^n \tag{2.10}$$

$$P = \begin{bmatrix}
1 & 26 & 66 & 26 & 1 & 0 & 0 & 0 & 0 \\
-5 & -50 & 0 & 50 & 5 & 0 & 0 & 0 & 0 \\
a_0 & b_0 & c_0 & d_0 & e_0 & 0 & 0 & 0 & 0 \\
0 & a_1 & b_1 & c_1 & d_1 & e_1 & 0 & 0 & 0 \\
0 & 0 & a_2 & b_2 & c_2 & d_2 & e_2 & 0 & 0 \\
\vdots & \vdots & \vdots & \vdots & \vdots & \vdots & \vdots & \vdots & \vdots \\
0 & 0 & 0 & 0 & -5 & -50 & 0 & 50 & 5 \\
0 & 0 & 0 & 0 & 1 & 26 & 66 & 26 & 1
\end{bmatrix}$$

$$Y = \left(w_0, w_1, w_2, \cdots, w_{n-1}, w_n\right)^{\mathrm{T}}$$

3. Stability Analysis

The Von Neumann technique will be used to investigate the stability of our system (2.8) as in [18] [19]:

$$\begin{aligned}
&a_i \omega_{i-2}^{n+1} + b_i \omega_{i-1}^{n+1} + c_i \omega_i^{n+1} + d_i \omega_{i+1}^{n+1} + e_i \omega_{i+2}^{n+1} \\
&= A_i \omega_{i-2}^{n} + B_i \omega_{i-1}^{n} + C_i \omega_i^{n} + D_i \omega_{i+1}^{n} + E_i \omega_{i+2}^{n}
\end{aligned}$$

Where $a_i, b_i, c_i, d_i, e_i, A_i, B_i, C_i, D_i$ and E_i given as (2.9):

To apply Von Neumann technique, we must linearize all of the nonlinear terms of system (2.9) by a local constant as follow:

$$\gamma_k + Z_k^2 = M_k, Z_k = N_k \tag{3.1}$$

According to the Von Neumann stability analysis, we have

$$\omega_i^n = \varepsilon^n \exp\left(q\phi ih\right) = \varepsilon^n \mathrm{e}^{q\phi ih}, q = \sqrt{-1} \tag{3.2}$$

where ϕ the waves number and h are the step size of *x*.

By substituting (3.2) in the system (2.8) with coefficients (2.9) we will get:

$$\begin{aligned}
&a_i \varepsilon^{n+1} \mathrm{e}^{q\phi(i-2)h} + b_i \varepsilon^{n+1} \mathrm{e}^{q\phi(i-1)h} + c_i \varepsilon^{n+1} \mathrm{e}^{q\phi(i)h} + d_i \varepsilon^{n+1} \mathrm{e}^{q\phi(i+1)h} + e_i \varepsilon^{n+1} \mathrm{e}^{q\phi(i+2)h} \\
&= A_i \varepsilon^{n} \mathrm{e}^{q\phi(i-2)h} + B_i \varepsilon^{n} \mathrm{e}^{q\phi(i-1)h} + C_i \varepsilon^{n} \mathrm{e}^{q\phi(i)h} + D_i \varepsilon^{n} \mathrm{e}^{q\phi(i+1)h} + E_i \varepsilon^{n} \mathrm{e}^{q\phi(i+2)h}
\end{aligned}$$

Dividing both sides of the last equation by $\varepsilon^n \mathrm{e}^{qi\phi h}$, we get the following relation:

$$\varepsilon\left(a\mathrm{e}^{-2q\phi h}+b\mathrm{e}^{-q\phi h}+c+d\mathrm{e}^{q\phi h}+e*\mathrm{e}^{2q\phi h}\right)$$
$$=A\mathrm{e}^{q-2\phi h}+B\mathrm{e}^{-q\phi h}+C+D\mathrm{e}^{q\phi h}+E\mathrm{e}^{2q\phi h}$$

So we can get the value of ε by the following relation:

$$\varepsilon=\frac{A\mathrm{e}^{q-2\phi h}+B\mathrm{e}^{-q\phi h}+C+D\mathrm{e}^{q\phi h}+E\mathrm{e}^{2q\phi h}}{a\mathrm{e}^{-2q\phi h}+b\mathrm{e}^{-q\phi h}+c+d\mathrm{e}^{q\phi h}+e*\mathrm{e}^{2q\phi h}}=\frac{Y}{X} \tag{3.3}$$

With linear coefficients:

$$a_i=\left(1-r_1M_k+r_2N_k+r_3\right),\quad A_i=\left(1+r_1M_k-r_2N_k-r_3\right)$$
$$b_i=\left(26-2r_1M_k+2r_2N_k-2r_3\right),\quad B_i=\left(26+2r_1M_k-2r_2N_k+2r_3\right)$$
$$c_i=\left(66-6r_2N_k\right),\quad C_i=\left(66+6r_2N_k\right)$$
$$d_i=\left(26+2r_1M_k+2r_2N_k+2r_3\right)\quad D_i=\left(26-2M_k-2r_2N_k-2r_3\right)$$
$$e_i=\left(1+r_1M_k+r_2N_k-r_3\right),\quad E_i=\left(1-r_1M_k-r_2N_k+r_3\right).$$

So we have:

$$\begin{aligned}X&=a\cos 2\phi h-qa\sin 2\phi h+b\cos\phi h-qb\sin\phi h+c\\&\quad+d\cos\phi h+qd\sin\phi h+e\cos 2\phi h+qe\sin\phi h\\Y&=A\cos 2\phi h-qA\sin 2\phi h+B\cos\phi h-qB\sin\phi h+c\\&\quad+D\cos\phi h+qD\sin\phi h+E\cos 2\phi h+qE\sin\phi h\end{aligned} \tag{3.4}$$

After substitution by the previous coefficients and simplifying the equation we get the final values of X and Y we get:

$$\begin{aligned}X&=\left[\left(2+2r_2N_k\right)\cos 2\phi h+\left(52+4r_2N_k\right)\cos\phi h+\left(66-6r_2N_k\right)\right]\\&\quad-q\left[\left(-2r_1M_k+2r_3\right)\sin 2\phi h+\left(-4r-1M_k-4r_3\right)\sin\phi h\right]\\Y&=\left[\left(2-2r_2N_k\right)\cos 2\phi h+\left(52-4r_2N_k\right)\cos\phi h+\left(66+6r_2N_k\right)\right]\\&\quad-q\left[\left(2r_1M_k-2r_3\right)\sin 2\phi h+\left(4r_1M_k+4r_3\right)\sin\phi h\right]\end{aligned} \tag{3.5}$$

We can put ε in the following form:

$$\varepsilon=\frac{Y}{X}=\frac{A+qB}{A^*+qB^*}$$

with

$$A=\left[\left(2-2r_2N_k\right)\cos 2\phi h+\left(52-4r_2N_k\right)\cos\phi h+\left(66+6r_2N_k\right)\right]$$
$$B=-\left[\left(2r_1M_k-2r_3\right)\sin 2\phi h+\left(4r_1M_k+4r_3\right)\sin\phi h\right]$$
$$A^*=\left[\left(2+2r_2N_k\right)\cos 2\phi h+\left(52+4r_2N_k\right)\cos\phi h+\left(66-6r_2N_k\right)\right]$$
$$B^*=\left[\left(2r_1M_k-2r_3\right)\sin 2\phi h+\left(4r+1M_k+4r_3\right)\sin\phi h\right]$$

It is very clear that X and Y are complex numbers so:

$$|\varepsilon|=\frac{\sqrt{A^2+B^2}}{\sqrt{A^{*2}+B^{*2}}} \tag{3.6}$$

It is clear that the value of $B=-B^*$ so $B^2=B^{*2}$ so the value of $|\varepsilon|$ depends only on the value of A^2 and A^{*2}, also the only condition that this method is stable that the value of $|\varepsilon| \le 1$, so we must proof that $A^2 \le A^{*2}$.

The previous condition is very difficult to prove but it is easy to prove that $A^2 = A^{*2}$ by taking the value of r_2 near zero and this happens when the value of (k) the step size of time (t) much less the value of (h) the step size of (x) as from Equation (2.5) the value of $r_2 = \frac{30k}{h^2}$.

This tends to reduce the step size of t to the maximum possible degree to guarantee stability.

4. Applications and Discussion

In this section, we apply the suggested method to solve STO equation with different initial value and exact solution, and we will show that our method produces a good approximation. Our proposed scheme's accuracy is measured by computing the l_2 error norm and maximum absolute error for several choices.

Error norms are defined as follows:

$$l_2 = \left\| u_{ex} - U_{app} \right\|_2 = \sqrt{h \sum_{i=0}^{n} \left| (u_i)_{ex} - (U_i)_{app} \right|^2},$$

$$l_\infty = \left\| u_{ex} - U_{app} \right\|_\infty = \max_{0 \le i \le n} \left| (u_i)_{ex} - (U_i)_{app} \right|.$$

The computations associated with the experiments were performed in the Mathematica software package.

Example 1: Consider Sharma-Tasso-Oliver Equation (STO) [23]

$$\frac{\partial U}{\partial t} + 3\alpha U_x^2 + 3\alpha U^2 U_x + 3\alpha U U_{xx} + \alpha U_{xxx} = 0$$

Subject to initial condition:

$$u(0,t) = \frac{1}{1 + e^{-x}}$$

The exact solution for this equation is given by:

$$U(x,t) = \frac{1}{1 + e^{-x+t}}$$

The numerical results are presented in **Tables 2-4** which show the comparison between the approximate solution and exact solution values at different values of $k = \Delta t$, within $\alpha = 1$, $h = \Delta x = 0.1$ and $k = \Delta t = 0.00000001$. **Table 5** show a comparison between the maximum absolute error and l_2 error norm at different values time levels. **Figures 1-3** show that the numerical approximate solution and exact solution are randomly same at different values of time. **Figure 4** shows the behavior of approximate solutions at different time levels.

Example 2: [23]

Consider the STO equation with different initial value and exact solution as follow:

$$\frac{\partial U}{\partial t} + 3\alpha U_x^2 + 3\alpha U^2 U_x + 3\alpha U U_{xx} + \alpha U_{xxx} = 0$$

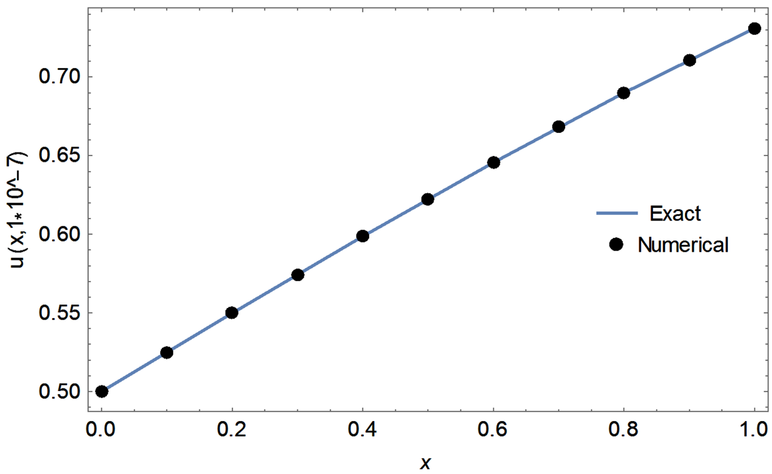

Figure 1. The behaviour of approximate and exact solutions at $t = 1.0 \times 10^{-7}$, $\alpha = 1$, $h = 0.1$ and $k = 0.00000001$.

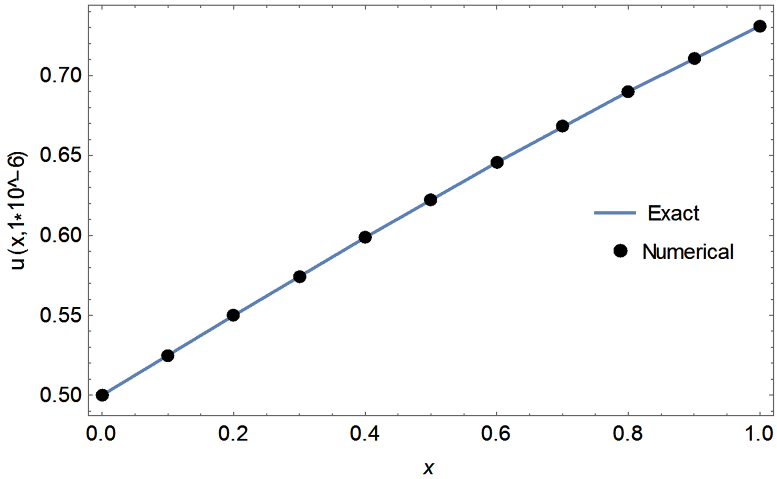

Figure 2. The behaviour of approximate and exact solutions at $t = 1.0 \times 10^{-6}$, $\alpha = 1$, $h = 0.1$ and $k = 0.00000001$.

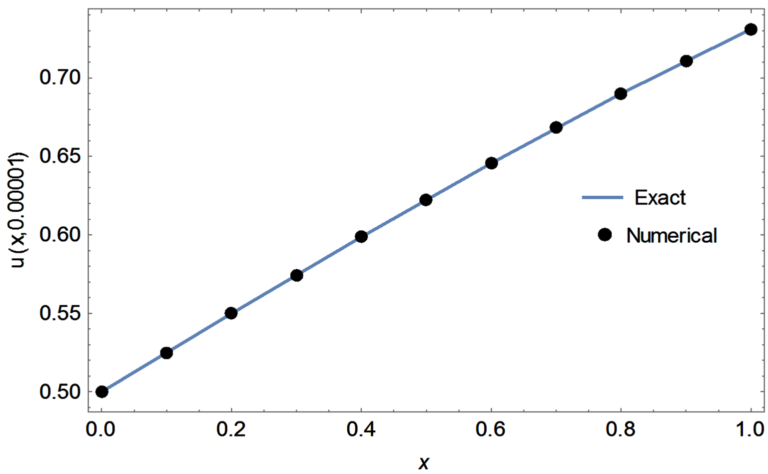

Figure 3. The behaviour of approximate and exact solutions at $t = 0.0001$, $\alpha = 1$, $h = 0.1$ and $k = 0.00000001$.

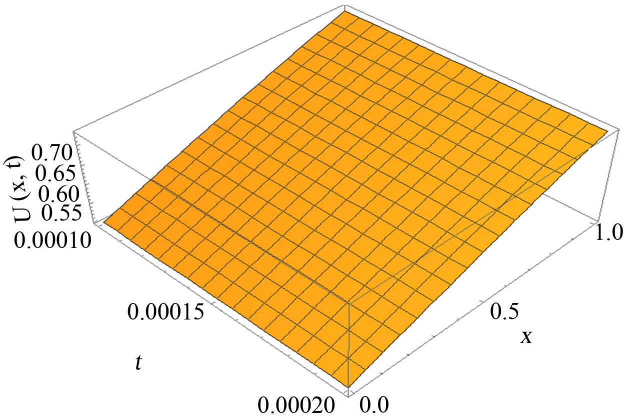

Figure 4. The behaviour of approximate solutions at different time levels when $\alpha = 1$, $h = 0.1$ and $k = 0.00000001$.

Table 2. Comprising between the approximate and exact solutions with errors at $t = 1.0 \times 10^{-7}$, $\alpha = 1$, $h = 0.1$ and $k = 0.00000001$.

x	Approximate	Exact	Error
0.1	0.5249791488547055	0.5249791625413359	1.36866×10^{-8}
0.2	0.5498339628667117	0.5498339725608206	9.69411×10^{-9}
0.3	0.5744424833260626	0.5744424923658276	9.03976×10^{-9}
0.4	0.5986876293875704	0.5986876360863772	6.69881×10^{-9}
0.5	0.6224593030471113	0.6224593077014831	4.65437×10^{-9}
0.6	0.6456562810552111	0.6456562833473711	2.29216×10^{-9}
0.7	0.6681877502916137	0.6681877499968785	2.94735×10^{-10}
0.8	0.6899744621041239	0.6899744597366424	2.36748×10^{-9}
0.9	0.7109494879255958	0.7109494820749729	5.85062×10^{-9}
1	0.7310585609349305	0.7310585589688111	1.96612×10^{-9}

Table 3. The Comprising between the approximate and exact solutions with errors at $t = 1.0 \times 10^{-6}$, $\alpha = 1$, $h = 0.1$ and $k = 0.00000001$.

x	Approximate	Exact	Error
0.1	0.5249788044652626	0.5249789381028935	1.33638×10^{-7}
0.2	0.5498336516535283	0.549833749795893	9.81424×10^{-8}
0.3	0.5744421824914142	0.5744422723533291	8.98619×10^{-8}
0.4	0.5986873525956109	0.5986874198516825	6.72561×10^{-8}
0.5	0.6224590498410654	0.6224590961981136	4.6375×10^{-8}
0.6	0.6456560542785053	0.6456560774415216	2.3163×10^{-8}
0.7	0.6681875538674655	0.6681875504552555	3.41221×10^{-9}
0.8	0.6899742898556037	0.6899742672178754	2.26377×10^{-8}
0.9	0.7109493583958809	0.7109492971246533	6.12712×10^{-8}
1	0.7310583839841464	0.7310583820180263	1.96612×10^{-9}

Table 4. The Comprising between the approximate and exact solutions with errors at $t = 0.0001$, $\alpha = 1$, $h = 0.1$ and $k = 0.00000001$.

x	Approximate	Exact	Error
0.1	0.5249753748166394	0.5249766937179152	1.3189×10^{-6}
0.2	0.5498305242370441	0.5498315221455173	9.97908×10^{-7}
0.3	0.5744391826314204	0.5744400722267223	8.89595×10^{-7}
0.4	0.5986845798180531	0.5986852575026235	6.77685×10^{-7}
0.5	0.6224565211257466	0.6224569811618548	4.6003×10^{-7}
0.6	0.6456537826134064	0.6456540183800584	2.357666×10^{-7}
0.7	0.6681855954511939	0.6681855550357042	4.04154×10^{-7}
0.8	0.6899725577174401	0.6899723420265835	2.15690×10^{-7}
0.9	0.7109480723990547	0.7109474476175955	6.2478×10^{-7}
1	0.7310566144722581	0.7310566125061296	1.9661×10^{-9}

Table 5. The obtained l_2 and l_∞ errors at different time steps $k = \Delta t$ and $\alpha = 1$, $h = 0.1$.

$k = \Delta t$	l_2 error norm	Max. abs. error
1×10^{-8}	1.24425×10^{-9}	2.50000×10^{-9}
5×10^{-8}	3.60618×10^{-9}	7.01476×10^{-9}
9×10^{-8}	6.28548×10^{-9}	1.23521×10^{-8}
1×10^{-7}	6.96308×10^{-9}	1.36862×10^{-8}
5×10^{-7}	3.43304×10^{-8}	6.70310×10^{-8}
9×10^{-7}	6.17481×10^{-8}	1.20322×10^{-7}
0.000001	6.86028×10^{-8}	1.33638×10^{-7}
0.000005	3.42689×10^{-7}	6.63631×10^{-7}
0.000009	6.16534×10^{-7}	1.18849×10^{-6}
0.0001	6.84959×10^{-7}	1.31890×10^{-6}

Subject to initial condition:

$$u(0,t) = -1 + \tanh(x)$$

The exact solution for this equation is given by:

$$U(x,t) = \frac{-2}{1 + \cosh(8t - 2x) - \sinh(8t - 2x)}$$

The numerical results are presented in **Tables 6-8** which show the comparison between the approximate solution and exact solution values at $\alpha = 1$, $h = \Delta x = 0.1$ and $k = \Delta t = 0.00000001$. **Table 9** shows a comparison between the maximum absolute error and l_2 error norm at different values time levels. **Figures 5-7** show that the numerical approximate solution and exact solution are randomly the same at different values of time. **Figure 8** shows the 3D behavior of approximate solutions at different time levels.

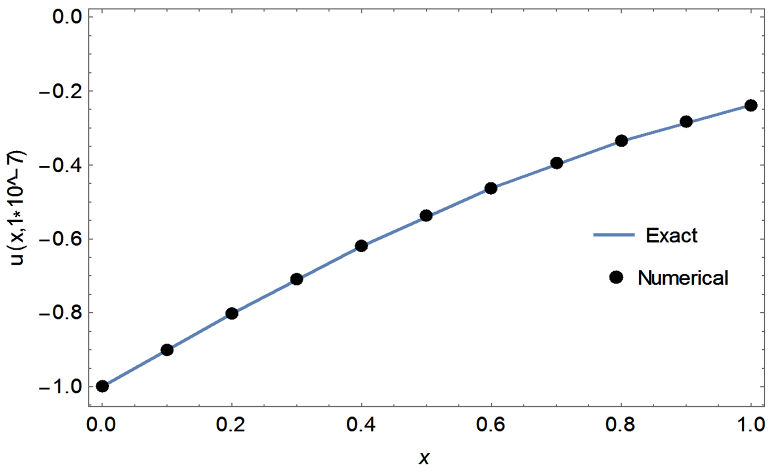

Figure 5. The behaviour of approximate and exact solutions at $t = 1\times10^{-7}$ with $\alpha = 1$, $h = 0.1$.

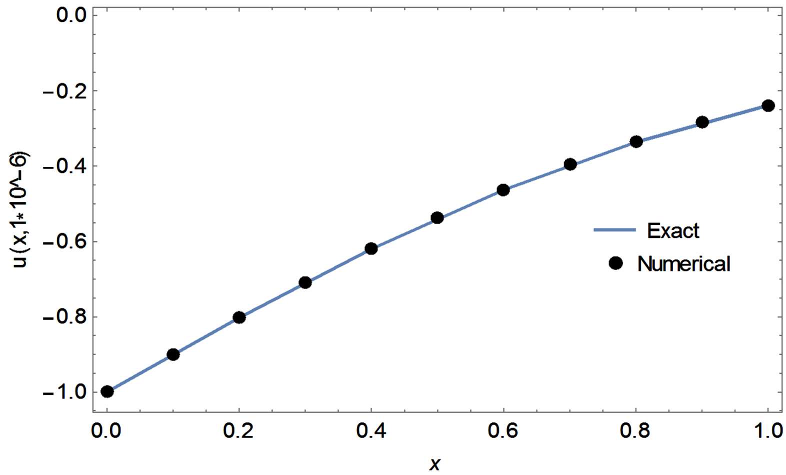

Figure 6. The behaviour of approximate and exact solutions at $t = 1\times10^{-6}$ with $\alpha = 1$, $h = 0.1$.

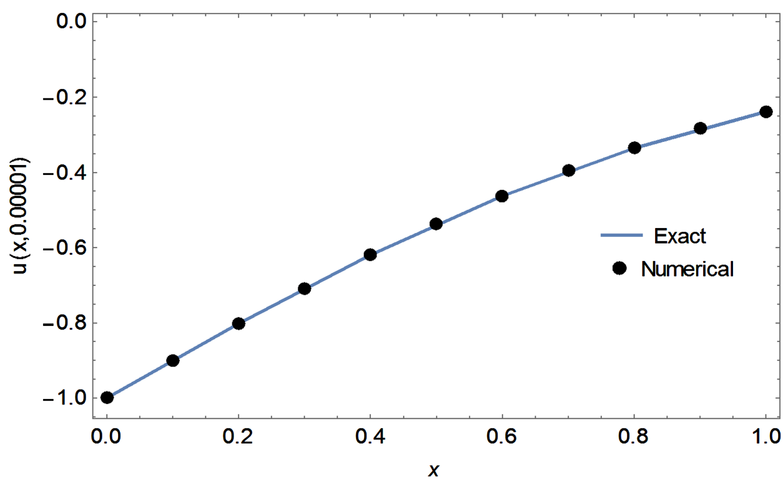

Figure 7. The behaviour of approximate and exact solutions at $\Delta t = 0.00001$ with $\alpha = 1$, $h = 0.1$.

Table 6. The comprising between the approximate and exact solutions with errors at $t = 1\times10^{-7}$ and $\alpha = 1$, $h = 0.1$.

X	Approximate	Exact	Error
0.1	−0.9003239011700949	−0.9003324014015763	8.50023×10^{-6}
0.2	−0.8026198749681477	−0.8026250641923195	5.18922×10^{-6}
0.3	−0.7086831923373599	−0.7086877536032365	4.56127×10^{-6}
0.4	−0.6200481204620889	−0.6200513800003417	3.25954×10^{-6}
0.5	−0.5378805844147091	−0.5378831573191416	2.5729×10^{-6}
0.6	−0.4629488207007662	−0.4629507176331309	1.89693×10^{-6}
0.7	−0.3956310142120661	−0.39563247677873387	1.46257×10^{-6}
0.8	−0.33596238431652836	−0.3359634533542775	1.06904×10^{-6}
0.9	−0.28370142511481006	−0.28370232456797584	8.9945×10^{-7}
1	−0.23840584404423507	0.23840601203402295	1.67989×10^{-7}

Table 7. The Comprising between the approximate and exact solutions with errors at $t = 1\times10^{-6}$ with $\alpha = 1$, $h = 0.1$.

X	Approximate	exact	Error
0.1	−0.9002504780675539	−0.9003359656417863	8.54875×10^{-6}
0.2	−0.8025767352176667	−0.8026285239500627	5.17887×10^{-6}
0.3	−0.708645412135447	−0.708691048100522	4.56359×10^{-6}
0.4	−0.6200218727210606	−0.620054460305121	3.25875×10^{-6}
0.5	−0.5378602548079978	−0.537885988536737	2.57337×10^{-6}
0.6	−0.46293432379048866	−0.4629532793191295	1.89555×10^{-6}
0.7	−0.39562010376657514	−0.3956347618473343	1.46580×10^{-6}
0.8	−0.3359548541057984	−0.3359654659587617	1.061185×10^{-6}
0.9	−0.28369486530106436	−0.2837040774760006	9.21217×10^{-7}
1	−0.2384073559560102	−0.23840752394671919	1.67990×10^{-7}

Table 8. The Comprising between the approximate and exact solutions with errors at $t = 0.00001$ with $\alpha = 1$, $h = 0.1$.

X	Approximate	exact	Error
0.1	−0.8995213036517695	−0.9003720042142316	8.50700×10^{-5}
0.2	−0.802128865390869	−0.8026635062211873	5.34640×10^{-5}
0.3	−0.7082701011953134	−0.7087243595167709	4.54258×10^{-5}
0.4	−0.6197534089903017	−0.6200856060823358	3.32197×10^{-5}
0.5	−0.537656212633913	−0.5379146158215734	2.58403×10^{-5}

Continued

0.6	−0.46278732644419796	−0.46297918136730526	1.91854×10^{-5}
0.7	−0.39550965012926387	−0.3956578669883961	1.48216×10^{-5}
0.8	−0.3358795169387979	−0.33598581616684337	1.062992×10^{-5}
0.9	−0.2836276012488011	−0.2837218018316331	9.42005×10^{-6}
1	−0.2384226435296663	−0.23842281152968955	1.6800002×10^{-7}

Table 9. The obtained l_2 and l_∞ errors on different time steps $k = \Delta t$.

$k = \Delta t$	l_2 **error norm**	**Max. abs. error**
1×10^{-7}	3.80932×10^{-6}	8.50023×10^{-6}
2×10^{-7}	7.62879×10^{-6}	1.70714×10^{-5}
3×10^{-7}	1.14465×10^{-5}	2.56274×10^{-5}
4×10^{-7}	1.52661×10^{-5}	3.41928×10^{-5}
5×10^{-7}	1.90832×10^{-5}	4.27431×10^{-5}
6×10^{-7}	2.29021×10^{-5}	5.13026×10^{-5}
7×10^{-7}	2.67184×10^{-5}	5.98472×10^{-5}
8×10^{-7}	3.05365×10^{-5}	6.84009×10^{-5}
9×10^{-7}	3.43519×10^{-5}	7.69394×10^{-5}
0.000001	3.81692×10^{-5}	8.54876×10^{-5}

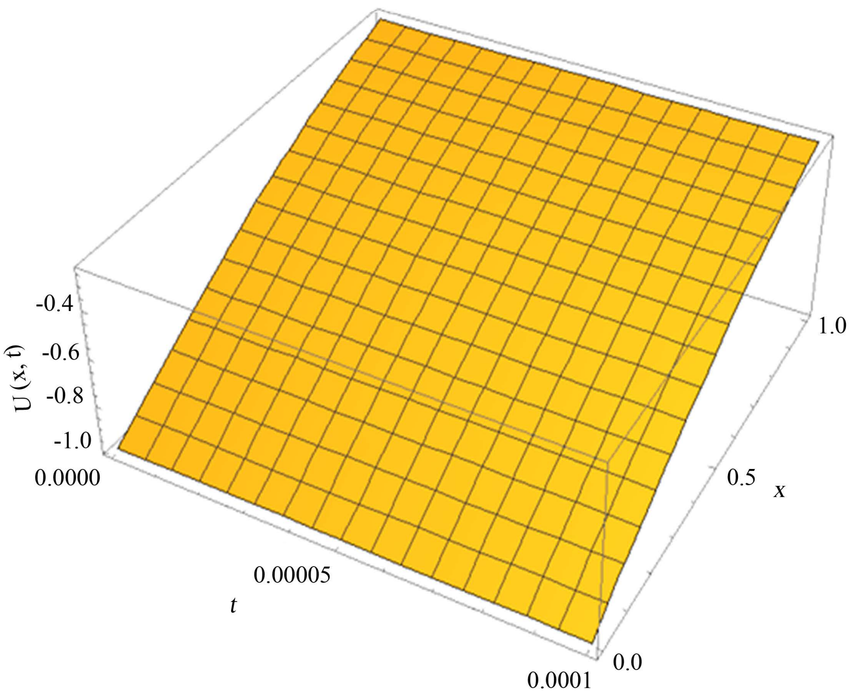

Figure 8. The 3D behaviour of approximate solutions at different time levels and $\alpha = 1$, $h = 0.1$.

5. Conclusion

The Quintic B-spline collocation method is used in this study to numerically solve the Sharma-Tasso-Olive equation. For the spatial variables and derivatives, we used quintic B-splines, which results in a set of first-order ordinary differential equations. The finite difference approach and the collocation method are the foundations of the developed plan for solving the problem under consideration. Analysis of stability demonstrated that the proposed scheme is infallibly stable. By calculating L_2 and L_∞ and comparing the error norms with past works, the precision and effectiveness of the proposed method have been demonstrated, and approximate solutions are explored. The acquired numerical results demonstrate the present method's remarkable performance as a numerical strategy for solving the (STO) problem and its applicability to a variety of situations.

Acknowledgements

The authors would like to express their sincere gratitude to the referees for the valuable suggestions to improve the paper.

Conflicts of Interest

The authors declare no conflicts of interest regarding the publication of this paper.

References

[1] Wazwaz, A.M. (2007) New Solitons and Kinks Solutions to the Sharma-Tasso-Olver Equation. *Applied Mathematics and Computation*, **188**, 1205-1213. https://doi.org/10.1016/j.amc.2006.10.075

[2] Yan, Z. (2003) Integrability for Two Types of (2 + 1)-Dimensional Generalized Sharma-Tasso-Olver Integro-Differential Equations, MMRC, AMSS. Academia Sinica, Beijing, 302-324.

[3] Lian, Z.-J. and Lou, S.Y. (2005) Symmetries and Exact Solutions of the Sharma-Tass-Olver Equation. *Nonlinear Analysis: Theory, Methods & Applications*, **63**, 1167-1177. https://doi.org/10.1016/j.na.2005.03.036

[4] Wang, S. Tang, X.-Y. and Lou, S.-Y. (2004) Soliton Fission and Fusion: Burgers Equation and Sharma-Tasso-Olver Equation. *Chaos, Solitons & Fractals*, **21**, 231-239. https://doi.org/10.1016/j.chaos.2003.10.014

[5] Wazwaz, A.-M. (2015) New Solutions for Two Integrable Cases of a Generalized Fifth-Order Nonlinear Equation. *Modern Physics Letters B*, **29**, Article ID: 1550065. https://doi.org/10.1142/S0217984915500657

[6] Yue, C. and Xia, T.C. (2014) Algebro-Geometric Solutions for the Complex Sharma-Tasso-Olver Hierarchy. *Journal of Mathematical Physics*, **55**, Article ID: 083511. https://doi.org/10.1063/1.4891605

[7] Lian, Z. and Lou, S.Y. (2005) Symmetries and Exact Solutions of the Sharma-Tasso-Olver Equation. *Nonlinear Analysis*, **63**, 1167-1177. https://doi.org/10.1016/j.na.2005.03.036

[8] Wang, M., Li, X. and Zhang, J. (2008) The $\left(\frac{G'}{G}\right)$-Expansion Method and Travel-

ling Wave Solutions of Nonlinear Evolution Equations in Mathematical Physics. *Physics Letters A*, **372**, 417-423. https://doi.org/10.1016/j.physleta.2007.07.051

[9] Klaus, M., Pelinovsky, D.E. and Rothos, V.M. (2006) Evans Function for Lax Operators with Algebraically Decaying Potentials. *Journal of Nonlinear Science*, **16**, 1-44. https://doi.org/10.1007/s00332-005-0652-7

[10] Zaki, S.I. (2000) Quintic B-spline Finite Elements Scheme for the KdVB Equation. *Computer Methods in Applied Mechanics and Engineering*, **188**, 121-134. https://doi.org/10.1016/S0045-7825(99)00142-5

[11] Mittal, R.C. and Jain, R.K. (2012) Application of Quintic B-Splines Collocation Method on Some Rosenau Type Nonlinear Higher Order Evolution Equations. *B Splines Based Solutions of Partial Differential Equations*, **13**, 42-152. https://doi.org/10.5899/2012/cna-00129

[12] Tariq, H. and Akram, G. (2016) Quintic Spline Technique for Time Fractional Fourth-Order Partial Differential Equation. *Numerical Methods for Partial Differential Equations*, **33**, 445-466. https://doi.org/10.1002/num.22088

[13] Jwamer, K.H.F. and Abdullah, N. (2016) Employment Higher Degree B-Spline Function for Solving Higher Order Differential Equations. *International Journal of Partial Differential Equations and Applications*, **4**, 16-19.

[14] Raslan, K.R., El-Danaf, T.S. and Ali, K.K. (2017) Collocation Method with Quintic B-spline Method for Solving Coupled Burgers' Equations. *Far East Journal of Applied Mathematics*, **96**, 55-75. https://doi.org/10.17654/AM096010055

[15] Ding, Q.X. and Wong, P.J.Y. (2020) Quintic Non-Polynomial Spline for Time-Fractional Nonlinear Schrödinger Equation. *Advances in Difference Equations*, **2020**, Article No. 577. https://doi.org/10.1186/s13662-020-03021-0

[16] Ahlberg, J.H., Nilson, E.N. and Walsh, J.L. (1967) The Theory of Splines and Their Applications. Mathematics in Science and Engineering: A Series of Monographs and Textbooks. 1st Edition, Academic Press, Cambridge, MA.

[17] Hamid, N.N.A., Majid, A.A. and Md Ismail, A.I. (2011) Extended Cubic B-Spline Method for Linear Two-Point Boundary Value Problems. *Sains Malaysiana*, **40**, 1285-1290.

[18] Al-Said, E.A., Noor, M.A., Almualim, A.H., Kokkinis, B. and Coletsos, J. (2011) Quartic Spline Method for Solving Second-Order Boundary Value Problems. *International Journal of Physical Sciences*, **6**, 4208-4212.

[19] Caglar, H., Caglar, N. and Elfaituri, K. (2006) B-Spline Interpolation Compared with Finite Difference, Finite Element and Finite Volume Methods which Applied to Two-Point Boundary Value Problems. *Applied Mathematics and Computation*, **175**, 72-79. https://doi.org/10.1016/j.amc.2005.07.019

[20] Fauzi, N.I.M. and Sulaiman, J. (2012) Half-Sweep Modified Successive over Relaxation Method for Solving Second Order Two-Point Boundary Value Problems Using Cubic Spline. *International Journal of Contemporary Mathmatices Sciences*, **7**, 1579-1589.

[21] Hadhoud, A.R., Abd Alaal, F.E., Abdelaziz, A.A. and Radwan, T. (2021) Numerical Treatment of the Generalized Time-Fractional Huxley-Burgers' Equation and Its Stability Examination. *Demonstratio Mathematica*, **54**, 436-451. https://doi.org/10.1515/dema-2021-0040

[22] Hadhoud, A.R., Alaal, F.E.A. and Abdelaziz, A.A. (2022) On the Numerical Investigations of the Time-Fractional Modified Burgers' Equation with Conformable Derivative, and Its Stability Analysis. *Journal of Mathematical and Computational Science*, **12**, 1-19. https://doi.org/10.28919/jmcs/6921

[23] Inc, M., Korpinar, Z.S., Al Qurashi, M.M. and Baleanu, D. (2016) A New Method for Approximate Solutions of Some Nonlinear Equations: Residual Power Series Method. *Advances in Mechanical Engineering*, **8**, 1-7. https://doi.org/10.1177/1687814016644580

[24] Kaya, D., Yokuş, A. and Demiroğlu, U. (2020) Comparison of Exact and Numerical Solutions for the Sharma-Tasso-Olver Equation. In: Machado, J., Özdemir, N. and Baleanu, D., Eds., *Nonlinear Systems and Complexity*, Springer, Cham. https://link.springer.com/chapter/10.1007/978-3-030-37141-8_3

[25] Alzaid, N. and Alrayiqi, B. (2019) Approximate Solution Method of the Seventh Order KdV Equations by Decomposition Method. *Journal of Applied Mathematics and Physics*, **7**, 2148-2155. https://doi.org/10.4236/jamp.2019.79147

[26] An, J. and Guo, X. (2021) Numerical Solution of Second-Orders Fuzzy Linear Differential Equation. *Applied Mathematics*, **12**, 1118-1125. https://doi.org/10.4236/am.2021.1211071